

# Direct Numerical Simulations of Fundamental Turbulent Flows with the Largest Grid Numbers in the World and its Application of Modeling for Engineering Turbulent Flows

Project Representative

Chuichi Arakawa Graduate School of Interdisciplinary Information Studies, The University of Tokyo

Authors

Chuichi Arakawa Graduate School of Interdisciplinary Information Studies, The University of Tokyo

Hiroshi Kawamura Department of Mechanical Engineering, Tokyo University of Science

Takashi Ishihara Graduate School of Engineering, Nagoya University

Yukio Kaneda Graduate School of Engineering, Nagoya University

In order to understand the statistics and physics of turbulence, we performed large-scale direct numerical simulations (DNS's) of canonical incompressible turbulent flows on the Earth Simulator (ES), including those of (i) turbulence in a periodic box with the number of grid points up to  $4096^3$ , (ii) channel turbulence with the number of grid points up to  $1024 \times 512 \times 1024$ , and (iii) turbulence in Ekman boundary layer with a code optimized by using HPF/ES. The DNS data were analyzed to study (i) the energy spectra in the near-dissipation wave number range and the energy transfer in the inertial sub-range, (ii) two-point velocity correlations in turbulent channel flows, and (iii) turbulence structures in Ekman boundary layer.

We also performed numerical simulations on the ES from the viewpoint of engineering applications. We made simulation of flows and acoustic fields around horizontal-axial-type of wind turbine by using compressible Large-Eddy simulation (LES), with emphasis on the blade tip region. Aerodynamic performance and acoustic emissions are predicted for the actual tip shape and an ogee type tip shape. These giant simulations are found to be available for the engineering topics such as design of wind turbine.

**Keywords:** incompressible turbulence, high-resolution DNS, channel turbulence, Ekman boundary layer, LES, wind turbine, noise reduction

## 1. Data analyses based on high-resolution DNS of incompressible turbulence

In order to study universal nature of fully developed turbulence at high Reynolds number, we have performed a series of direct numerical simulations (DNS's) of forced incompressible turbulence in a periodic box with the number of grid points from  $256^3$  to  $4096^3$  on the Earth Simulator (ES). We set the values of kinematic viscosity  $\nu$  and the maximum wave number  $k_{\max}$  so that  $k_{\max}\eta \sim 1$  in Series 1 and  $k_{\max}\eta \sim 2$  in Series 2, where  $\eta$  is the Kolmogorov dissipation length scale. The attained Taylor micro-scale Reynolds number  $R_\lambda$  ranges from 167 to 1131 in Series 1 and from 94 to 675 in Series 2 [1, 2]. The DNS data have potential ability to elucidate the universal nature of high Reynolds number turbulence. Recently we have also performed a series of DNS's of incompressible channel turbulence. The number of grid points is up to  $1024 \times 512 \times 1024$ . The attained maximum friction Reynolds number  $Re_\tau$  is about 1300. Here we present some results obtained by the

recent analyses of these DNS data.

### 1.1. Data analyses based on the high-resolution DNS of box turbulence

#### 1.1.1. Energy spectrum in the near dissipation range

By using the DNS data in series 2, we studied the energy spectrum in the near dissipation range (DR). According to the Kolmogorov hypotheses the energy spectrum is universal in the equilibrium range, and experiments as well as DNS suggest that the effect of intermittency on the energy spectrum is weak even if it exists. It has been suggested from previous studies that DNS spectra for  $R_\lambda < 100$  fit well to the form  $E(k) = C(k\eta)^\alpha \exp(-\beta k\eta)$  in the near DR, where  $C$ ,  $\alpha$  and  $\beta$  are constants independent of  $k$ . Our analysis suggests that (i) the DNS spectra for  $94 < R_\lambda < 675$  continue to fit well to the form in the near DR ( $0.5 < k\eta < 1.5$ ), (ii) the values of  $\alpha$  and  $\beta$  decrease monotonically with  $R_\lambda$ , and (iii) they approach to  $R_\lambda$ -independent constants as  $R_\lambda$  goes to infinity, in accordance with the Kolmogorov hypotheses, but the

approach, especially that of  $\beta$ , is very slow. For example, according to a curve fitting based on the DNS data,  $|\beta(R_\lambda) - \beta(R_\lambda = \text{infinity})| / \beta(R_\lambda = \text{infinity})$  is still as large as 2.61, even at  $R_\lambda = 10,000$  [1].

### 1.1.2. Energy transfer in the inertial subrange

We also studied the statistics of energy transfer by using the data of a series of high-resolution DNS's of incompressible homogeneous turbulence in a periodic box. The data show that the energy transfer  $T$  through the wave number  $k$  is highly intermittent and the skewness  $S$  and flatness  $F$  of  $T$  increase with  $k$  approximately as  $S \sim (kL)^\alpha$  and  $F \sim (kL)^\beta$  in the inertial subrange, where  $\alpha \sim 2/3$ ,  $\beta \sim 1$  and  $L$  is the characteristic length scale of energy containing eddies. The relation between the statistics of  $T$ , the energy dissipation rate  $\varepsilon$  and its average  $\varepsilon_r$  over a domain of scale  $r$  is also studied;  $T$  is less intermittent than  $\varepsilon_r$  but there is similarity to a certain degree in their probability distribution functions.

### 1.2. DNS of channel turbulence

We studied two-point velocity correlations by using the DNS data of turbulent channel flow with  $Re_\tau \sim 1300$ . In turbulent channel flow, two-point velocity correlations depend on the direction of the velocity, the distance vector between the two points, the distance of the two points from the wall, as well as the friction Reynolds number. Here we focused on the integral length scale ( $L$ ), the Taylor micro-scale ( $\lambda$ ) and the Kolmogorov dissipation length scale ( $\eta$ ), which characterize the two-point velocity correlations. The data show that  $L$  as well as  $\lambda$  is proportional to  $(y^+)^\alpha$  in the log layer ( $30 < y^+ < 500$ ), where  $y$  is the distance from the wall and a  $+$  superscript denotes that the quantities are normalized with the friction velocity  $u_\tau$  and the viscous length scale  $\delta_\tau = \nu / u_\tau$ . The data also show that  $\eta^+$  approaches to a theoretical prediction  $\eta^+ \sim (\kappa y^+)^{1/4}$  with  $\kappa \sim 0.4$  in the log layer for large  $Re_\tau$ . We have also studied the  $y^+$ -dependence of Taylor micro-scale Reynolds numbers ( $R_\lambda$ ). The data shows that the maximum  $R_\lambda$  in the channel turbulence with  $Re_\tau \sim 1300$  is about 170 at  $y^+ \sim 600$ . In spite of the relatively large number of grid points (1024x512x1024), the attained Taylor micro-scale Reynolds number is small in channel turbulence as compared to those attained by the ultra-scale DNSs of box turbulence. This fact and our experience in high-resolution DNS of box turbulence suggest that much higher-resolution is necessary for the study of asymptotic nature of turbulent channel flows at high Reynolds number by DNS.

## 2. DNS of the turbulent Ekman boundary layer

Rotation is one of the key factors that affect the planetary boundary layer (PBL). The boundary layer under the effect of the system rotation is called as the Ekman boundary layer. The Ekman boundary layer exists in the PBL. The works on

the laminar PBL have been widely performed mainly by the theoretical methods. On the other hand, Large-Eddy simulation (LES) and Reynolds Averaged Navier-Stokes equation (RANS) have been the major tools in most numerical researches on the turbulent PBL, since the turbulent PBL is much more complex and it includes from small-scale motions to very large-scale ones. The DNS of the turbulent Ekman boundary layer provides fundamental information on the three-dimensional turbulent boundary layer and the PBL in order to improve turbulence models in LES and RANS.

Among studies of the Ekman boundary layer, the researches using the DNS have barely been performed. Coleman [3] conducted the DNS of the turbulent Ekman boundary layer with a high Reynolds number of  $Re_f = 1000$ . However, the turbulent structure in the upper region was not discussed, because the computational domain was small.

In the present study, we calculated the neutrally stratified turbulent Ekman boundary layer with a higher Reynolds number of  $Re_f = 1140$ , and examined the three-dimensional characteristics in the turbulent Ekman boundary layer.

### 2.1. Numerical procedures

The flow field is the turbulent Ekman boundary layer of an incompressible viscous fluid over a smooth flat surface. The system is rotating about a vertical axis. The flow is driven by the combination of the horizontal pressure gradient and the Coriolis force. The periodic boundary conditions are imposed in the horizontal directions. The non-slip and the Neuman conditions are adapted at the lower and upper boundaries, respectively. The governing equations are the continuity equation and the Navier-Stokes equation. The Reynolds number are set to be  $Re_f = 400, 510, 600, 775$  and 1140.

In the present computation, the fractional step method is adopted for the coupling between the continuity and the Navier-Stokes equations. The second-order Crank-Nicolson and the Adams-Bashforth methods are employed as the time advance algorithms, the former for the vertical viscous term and the latter for the other terms. The finite-difference method is used for the spatial discretization. The fourth-order central difference scheme is adapted in the streamwise and spanwise directions, and the second-order central difference scheme is used in the wall-normal direction.

The non-dimensional parameters are the Reynolds number ( $Re$ ) and the Rossby number ( $Ro$ ). They are defined by  $Re = Gh / \nu$  and  $Ro = G / fh$ , respectively.

### 2.2. Results

The absolute values of mean velocity  $Q^+$  as a function of the height  $y^+$  are given in figure 1 and compared with the experiments of Caldwell *et al.* [4]. The DNS of turbulent Ekman boundary layer performed by Coleman [3] and the

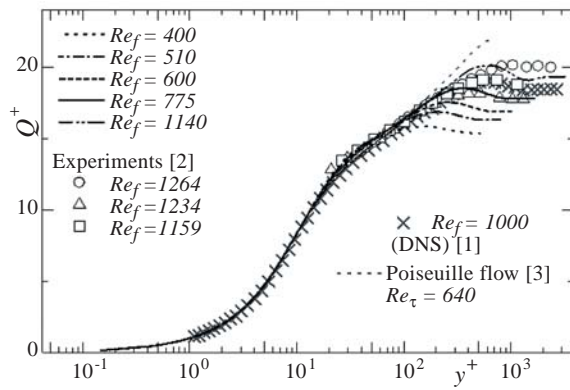


Fig. 1 Mean velocity profiles.

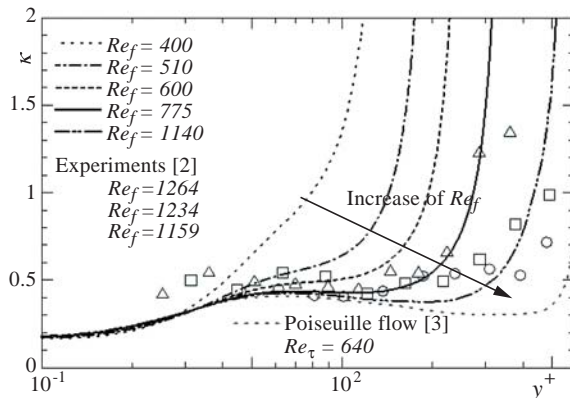


Fig. 2 The von Karman constant

one of the turbulent Poiseuille flow by Abe *et al.* [5] are also shown for comparison.

It is well known that in the wall turbulence, the mean velocity follows the logarithmic region. In the cases of  $Re_f = 400$  and  $510$ , the logarithmic region is not observed. On the other hand, in the cases of  $Re_f = 600, 775$  and  $1140$  the logarithmic region appears in the region of  $y^+ > 30$ . Present results with  $Re_f = 775$  and  $1140$  well agree with the experiments of Caldwell *et al* [4]. and the DNS of Coleman [3].

The von Karman constants  $\kappa$  are shown in figure 2. In the cases of  $Re_f = 400, 500$  and  $600$ ,  $\kappa$  does not exhibit any constant region but increases monotonically. In the higher Reynolds number of  $Re_f = 775$ ,  $\kappa$  starts to show a constant region. With further increase of Reynolds number,  $\kappa$  exhibits a local maximum and stays almost constant in a wider range of the distance from wall. This trend is very close to the one obtained for the turbulent Poiseuille flow [5].

Existence of the large-scale structures in the wall turbulence with high Reynolds numbers has been reported recently. Several DNS's of turbulence with simple boundary condition such as the turbulent channel flow are being made in order to obtain detail information about the large-scale structures.

The instantaneous flow filed for  $Re_f = 1140$  is illustrated in figure 3. The iso-surfaces colored by red and blue show

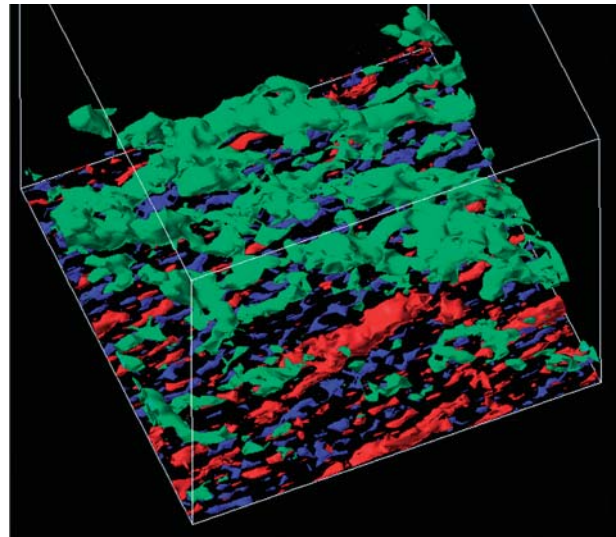


Fig. 3 Bird's eye view of instantaneous flow filed for  $Re_f = 1140$ . Red, high-speed regions,  $u'^+ > 3.0$ ; blue, low-speed regions,  $u'^+ < -3.0$ ; Light green, low-speed regions,  $u'^+ < -1.0$ , in upper region.



Fig. 4 WIDMELIII

the high ( $u'^+ > 3.0$ )- and low-speed region ( $u'^+ < -3.0$ ), respectively. The light green iso-surfaces show low-speed region ( $u'^+ < -1.0$ ). Here, the velocity fluctuation  $u'$  means the fluctuation parallel to the mean velocity direction at each height. In the vicinity of the wall, the well-known streak structures are observed. In the upper region, the large low-speed region exists, which inclines against the direction of mean flow velocity.

### 3. Numerical Approach for Noise Reduction of Wind Turbine Blade Tip

The purpose of this giant simulation is to investigate the physical mechanisms associated with tip vortex noise caused by rotating wind turbines. The flow and acoustic field around the horizontal axial type of wind turbine WINDMELL III shown in Fig. 4 was simulated using compressible Large-Eddy simulation (LES), with emphasis on the blade

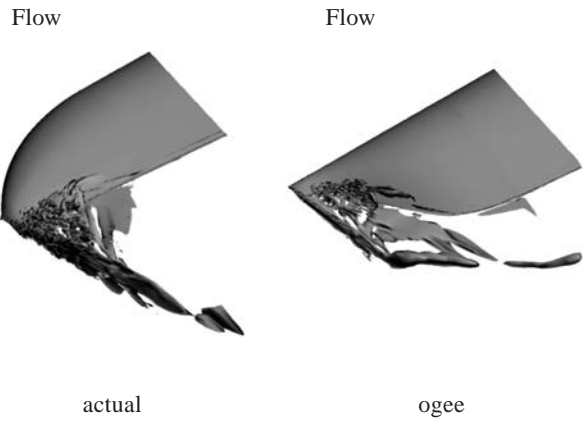


Fig. 5 Vorticity  $\omega_x$  isosurfaces.

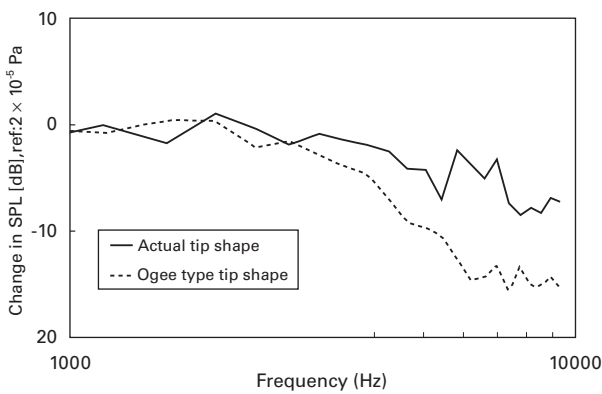


Fig. 6 Sound pressure level – Simulation results.

tip region. The acoustic near field was simulated directly by LES whereas the far field was modeled using acoustic analogy. The broadband noise was predicted by splitting the computational domain into 2 parts: the near field and the far field. The propagation of acoustic waves in the near field was simulated directly by LES while the noise in the far field was modeled by Ffowcs Williams-Hawkings equations. Due to the fine grid of 300 million employed, smallest eddy scales near the blade surface were resolved and described in Fig. 5. Aerodynamic performance and acoustic emissions were predicted for the actual tip shape and an ogee type tip shape. At a distance of 20 m, the use of an ogee type tip shape can reduce the noise level for frequencies above 4 kHz by up to 5 dB. Fig. 6 shows that a decrease of the sound pressure level in the high frequency domain was observed for the ogee type tip shape. The new figure of tip shape,

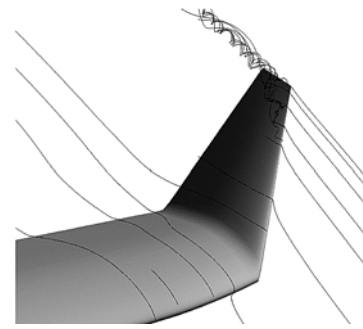


Fig. 7 New trial of winglet for rotating proplellar

which was generally called as winglet in the airplane shown in Fig. 7, was also investigated with this simulation code for the further development of high efficiency turbine. The design of optimized tip shapes for reduction of wind turbine noise emission is essential as it can improve public acceptance of wind energy.

### References

- [1] Y. Kaneda, T. Ishihara, M. Yokokawa, K. Itakura, and A. Uno, "Energy dissipation rate and energy spectrum in high resolution direct numerical simulations of turbulence in a periodic box" *Phys. Fluids*, 15 (2), (2003) L21-L24.
- [2] T. Ishihara, Y. Kaneda, M. Yokokawa, K. Itakura, and A. Uno, "Energy Spectrum in the Near Dissipation Range of High Resolution Direct Numerical Simulation of Turbulence" *J. Phys. Soc. Jpn.* 74 (5), (2005) to appear.
- [3] G. N. Coleman, "Similarity statistics from a direct numerical simulation of the neutrally stratified planetary boundary layer", *J. Atmos. Sci.*, 56, (1999) 891-900.
- [4] Caldwell *et al.*, "A laboratory study of the turbulent Ekman layer", *Geophys. Fluid Dyn.*, 3, (1972) 125-160.
- [5] Abe, H., Kawamura, H. & Matsuo, Y., "Direct numerical simulation of a fully developed turbulent channel flow with respect to the Reynolds number dependence", *Trans. ASME J. Fluids Eng.*, 123, (2001) 382-393.
- [6] C. Arakawa, O. Fleig, M. Iida and M. Shimooka, "Numerical Approach for Noise Reduction of Wind Turbine Blade Tip with Earth Simulator", *Journal of the Earth Simulator*, 2, (2005), 11-33.

# 乱流の世界最大規模直接計算とモデリングによる応用計算

プロジェクト責任者

荒川 忠一 東京大学 大学院情報学環

著者

荒川 忠一 東京大学 大学院情報学環

河村 洋 東京理科大学 理工学部 機械工学科

石原 卓 名古屋大学大学院工学研究科

金田 行雄 名古屋大学大学院工学研究科

乱流の統計と物理を理解するため、地球シミュレータ(ES)を用いて、非圧縮性乱流のいくつかのカノニカルな問題に対する大規模直接数値計算(DNS)を行った。具体的には、(i)最大格子点数 $4096^3$ の周期的乱流、(ii)最大格子点数 $1024 \times 512 \times 1024$ のチャンネル乱流、(iii)エクマン境界層の乱流である。これらのDNSにより得られたデータを解析した結果、(i)では、散逸領域におけるエネルギースペクトルがある関数形でよくフィットできるが、その関数を定めるパラメータの $Re \rightarrow \infty$ での収束が非常に遅いこと、及び、慣性小領域のスケールにおけるエネルギー輸送のSkewnessやFlatnessがあるべき側に従うこと等が分かった。また(ii)では、乱流境界層における2点速度相関を特徴つける積分長やTaylorマイクロスケール( $\lambda$ )が慣性低層において壁からの距離のべき則に従うこと、及び、 $Re_\tau=1300$ の比較的大規模な壁乱流DNSにおいても、Taylorマイクロスケールに基づくレイノルズ数 $Re_\lambda$ は高々170(周期的乱流の $256^3$ 相当)であることが分かった。また、(iii)では、エクマン境界層の乱流においては世界最大規模のDNSを実現した。これにより、レイノルズ数増大と共に対数領域が現れ、さらにカルマン定数がポアズイユ乱流の分布に近づく傾向を確認した。また、壁から離れた領域において大規模な低速領域が存在することを確認した。なお、用いたコードはHPF/ESによりES用に最適化したものである。

我々はまた工学的応用の立場からの数値計算もES上でやっている。特に、格子点数3億点のオーダーの大規模LES解析では、プロペラ風車の翼端を中心とした詳細な流体力学および騒音解析を同時に行うことを可能とした。それを用いて通常の翼先端と、騒音が小さくなるといわれているS形状をした“Ogee”タイプを比較し、“Ogee”タイプの翼先端形状は通常の翼先端と比較して、5 dBほど騒音が小さいことを定量的に示すことに成功した。

キーワード:非圧縮性乱流, 大規模直接数値計算, チャンネル乱流, エクマン境界層, ラージ・エディ・シミュレーション, 風車, 騒音